This is the accepted manuscript made available via CHORUS. The article has been published as:

Measurement of the magnetic penetration depth of a superconducting MgB_{2} thin film with a large intraband diffusivity

Jeehoon Kim, N. Haberkorn, Shi-Zeng Lin, L. Civale, E. Nazaretski, B. H. Moeckly, C. S. Yung, J. D. Thompson, and R. Movshovich

Phys. Rev. B **86**, 024501 — Published 5 July 2012
DOI: 10.1103/PhysRevB.86.024501

Measurement of the magnetic penetration depth of a superconducting MgB_2 thin film with a large intraband diffusivity

Jeehoon Kim,[1,*] N. Haberkorn,[1] Shi-Zeng Lin,[1] L. Civale,[1] E. Nazaretski,[2]
B. H. Moeckly,[3] C. S. Yung,[3] J. D. Thompson,[1] and R. Movshovich[1]

[1]*Los Alamos National Laboratory, Los Alamos, NM 87545*
[2]*Brookhaven National Laboratory, Upton, NY 11973*
[3]*Superconductor Technologies Inc., Santa Barbara, CA 93111*

(Dated: June 12, 2012)

We report the temperature dependent magnetic penetration depth $\lambda(T)$ and the superconducting critical field $H_{c2}(T)$ in a 500-nm MgB_2 film. Our analysis of the experimental results takes into account the two gap nature of the superconducting state and indicates larger intraband diffusivity in the three-dimensional (3D) π band compared to that in the two-dimensional (2D) σ band. Direct comparison of our results with those reported previously for single crystals indicates that larger intraband scattering in the 3D π band leads to an increase of λ. We calculated λ and the thermodynamic critical field $H_c \approx$2000 Oe employing the gap equations for two-band superconductors. Good agreement between the measured and calculated λ value indicates the two independent measurements, such as magnetic force microscopy and transport, provide a venue for investigating superconducting properties in multi-band superconductors.

I. INTRODUCTION

During the last decade a significant effort has been made to understand the mechanism of two-band superconductivity in MgB_2.[1–4] MgB_2 has two s-wave gaps residing on four different disconnected Fermi surface (FS) sheets: two axial quasi two-dimensional (2D) σ-band sheets and two contorted three-dimensional (3D) π-band sheets. The σ band forms two concentric cylindrical sheets via in-plane sp^2 hybridization of the boron valence electrons. The π band results from the strongly coupled covalent bonding and antibonding of the boron P_z orbitals.[5] Multiple bands allow for both inter- and intraband scattering. It is thus possible to tune the upper critical field (H_{c2}) via doping, which has different effects on the inter- and intra-band scattering strengths.[2,6–8] In MgB_2 the anisotropy of the temperature dependent penetration depth λ, $\gamma_\lambda(T) = \lambda_c(T)/\lambda_{ab}(T)$ shows remarkably different behavior compared to that of H_{c2}, $\gamma_{H_{c2}}(T) = H^{ab}_{c2}(T)/H^{c}_{c2}(T)$.[9,10] This difference indicates that the two-band nature of superconductivity profoundly alters the superconducting properties compared to those in a single band material.[11] For example, the equations for critical fields and depairing current as a function of λ and ξ should be modified due to the inter/intra-band scattering. Knowledge of the absolute values of λ and ξ is also important for technological applications.[12] For example, the acceleration field in superconducting radio frequency (SRF) cavities could be enhanced by covering conventional superconducting Nb cavities with superconductor/insulator multilayers (such as MgB_2) with higher thermodynamic critical field (H_c).[13]

A number of measurements have been performed to determine the absolute value of λ in MgB_2.[3,9,10] The reported values of λ range from 40 nm to 200 nm, indicating that λ is strongly affected by inter- and intra-band scattering.[14–20] In this paper we present measurements of the absolute values of $\lambda(T)$, employing low temperature magnetic force microscopy (MFM), and of the angular-dependent $H_{c2}(T,\theta)$ performed via electrical transport, in a 500-nm thick MgB_2 film. Our MgB_2 film can be described by the dirty limit two-band Usadel equations. We analyze the measured values of H_{c2} and λ using a model developed for dirty superconductors,[2] which simplifies the analysis compared to that reported in Ref. 15. We investigate theoretically the influence of the inter/intra-band scattering on the superconducting properties. Using a two-band superconductor model with parameters obtained from a fit to $H_{c2}(T,\theta)$, we calculate λ and H_c which are consistent with the experimental values.

II. EXPERIMENT

A MgB_2 film was grown on a r-sapphire substrate by a reactive evaporation technique.[21,22] The film is epitaxial and shows columnar growth morphology, with the c axis tilted by a few degrees from the normal direction of the substrate. For more details see Ref. 22. The sample has dimensions L=4 mm $\times$ W=5 mm $\times$ t=500 nm, and exhibits a full superconducting volume fraction based on measurements using a commercial SQUID magnetometer (Quantum Design magnetic property measurement system, MPMS) All MFM measurements described here were performed in a home-built low temperature MFM apparatus.[23] Temperature dependent vortex images were taken in the frequency-modulated mode after a small magnetic field was applied above T_c (field-cooled). We used high resolution SSS-QMFMR cantilevers.[24] The magnetic field was always applied perpendicular to the film surface and parallel to the MFM tip. The absolute values of $\lambda(T)$ were determined by comparing the Meissner response curves with those for a reference sample at

4 K.[25,26] The Meissner technique for the λ measurement was first proposed by Xu *et al.*[27] and demonstrated by Lu *et al.*[28] The film thickness of 500 nm is larger than $\lambda \approx$ 200 nm, which makes corrections to λ due to the sample thickness insignificant. Conventional four-lead resistivity measurements used for determining $H_{c2}(T, \theta)$, where θ is an angle between the applied magnetic $\mathbf{H}$ and the crystallographic c axis, were performed with a rotatable probe in a commercial Quantum Design physical property measurement system (PPMS), in magnetic fields between 0 T and 9 T. The superconducting critical temperature T_c = 38.3 K (zero resistance) and the transition width ΔT_c = 0.5 K were determined from the transport measurements. Zero-field-cooling measurements at the MPMS with $H \approx$1 Oe show T_c=38.0 K. The small value of residual resistivity ratio (RRR$\approx$4) indicates the presence of impurities, consistent with the dirty limit.

III. RESULTS AND DISCUSSION

A. MFM measurements in the MgB_2 film

Figure 1(a) presents a typical vortex image in the MgB_2 thin film. The well-formed vortices in the 6 μm $\times$ 6 μm field of view were observed, which suggests the homogeneity of the sample on a micron scale. However, the irregular shape of individual vortices suggests the presence of inhomogeneity in the superfluid density on a sub-micron scale, which may be related to impurities. Figures 1(b) and (c) show MFM images of isolated vortices in MgB_2 at 4 K and 15 K, respectively. The features besides a single vortex represent a sub-micron scale inhomogeneity, indicating small variations of superfluid density. Figure 1(d) depicts a line profile taken along the dotted line in Figs. 1(b) and (c) for each of the vortices. The maximum force gradient $[max(\partial f/\partial z)]$ at the center of the vortex qualitatively indicates that the magnitude of λ at 15 K is larger than that at 4 K.[29–31] In order to determine the absolute value of λ, we performed Meissner experiments. The force between the tip magnetic moment (a distance d above the sample) and the shielding currents induced by the tip field is equal to the force between the real tip and the image tip, with the mirror plane at a distance λ below the sample's surface.[32] This force therefore is a function of $d + \lambda$ when $d \gg \lambda$. Direct comparison of the Meissner curves taken at 4 K for MgB_2 and a reference sample (Nb) with a known λ gives λ(4 K) = 200 ± 30 nm for MgB_2.[25] Comparing Meissner curves for MgB_2 at 4 K and at a given temperature T yields $\delta\lambda(T)$. We obtain the absolute value of the temperature dependent $\lambda(T)$ by adding $\delta\lambda(T)$ to λ(4 K). Figure 2(a) shows the Meissner force response as a function of the tip-sample distance at several temperatures. The systematic evolution of the Meissner response with respect to temperature reflects the change of λ with temperature. Figure 2(b) shows the normalized $\lambda(T)$ (black squares) obtained for MgB_2 using the procedure outlined above,

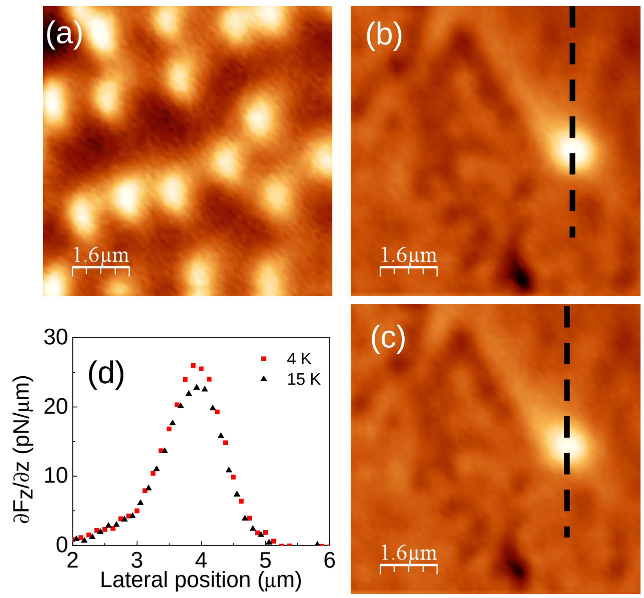

FIG. 1: (Color online) (a) A typical vortex image with a tip-lift height of 300 nm in the MgB_2 thin film. (b) and (c) Single vortex images with a tip-lift height of 300 nm, acquired at T = 4 K and T = 15 K, respectively. (d) The single vortex profile along the dotted lines in (b) and (c). Higher peak value corresponds to a smaller λ value.

deviating significantly from the BCS theory curve (the red dashed line), which is consistent with the previous studies shown as green solid circles.[10] This discrepancy indicates a profound effect of two-band superconductivity in MgB_2.[10] The large λ in MgB_2 may be due to inclusion of impurities, such as C, N, and Al, which significantly affects the electron mean-free path in each band of MgB_2.

B. H_{c2} measurements in the MgB_2 film

In order to investigate the nature of disorder, we performed temperature dependent H_{c2} measurements. Figure 3(a) shows $H_{c2}(T)$ with the field parallel to the c axis $H_{c2}^{\parallel c}(T)$ (black circles). The value of $H_{c2}(0)$ is considerably higher than that found in clean single crystals ($H_{c2}^{\parallel c}(0) \approx$ 3-5 T)[33], which indicates that the film is in the dirty limit. The Gurevich model for two-band superconductors[2] considers inter- and intra-band scattering by non-magnetic impurities in the dirty limit. The high T_c in our film (which shows essentially no suppression compared to the clean crystals) is consistent with a small inter-band scattering, so we can use the equations obtained for $H_{c2}(T)$ neglecting the inter-band scattering:

$$\begin{aligned} &a_2[\ln(t) + U(\eta h)] + a_1[\ln(t) + U(h)] \\ &+a_0[\ln(t) + U(h)][\ln(t) + U(\eta h)] = 0, \end{aligned} \tag{1}$$

where $U(x) = \psi(1/2 + x) - \psi(1/2)$, $\psi(x)$ is the digamma function, $a_1 = 1 + L_-/L_0$, $a_2 = 1 - L_-/L_0$,

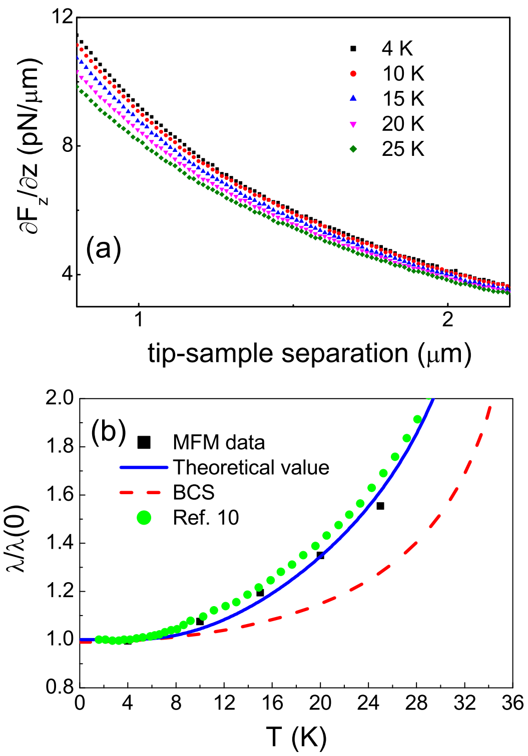

FIG. 2: (Color online) (a) Temperature dependence of the Meissner response in MgB_2. (b) $\lambda(T)$ marked by the black squares are inferred from the data shown in (a). The blue solid curve shows the calculated $\lambda(T)$ from the gap equations for two-band superconductors. The red dashed curve represents the conventional BCS model. The green circles are taken from tunnel diode resonator measurements (Ref. 10).

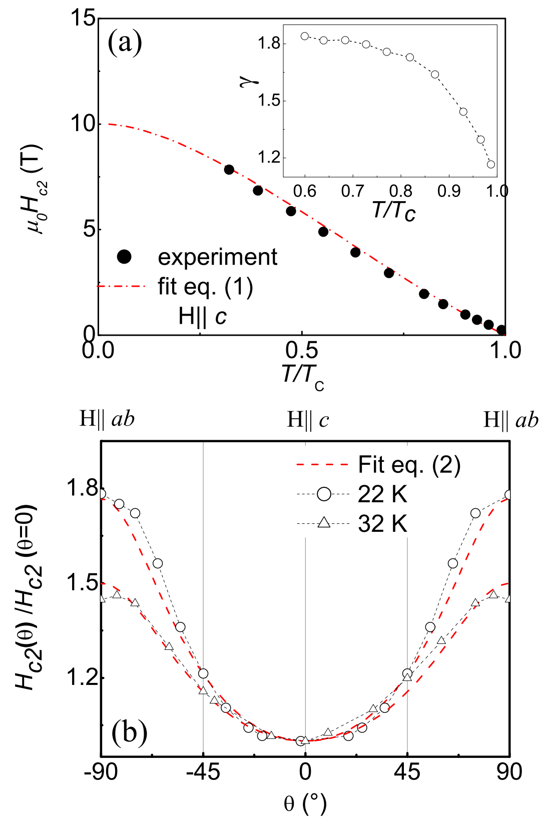

FIG. 3: (Color online) (a) Numerical fit to $H_{c2}(T)$ obtained from transport data. The inset shows the temperature dependence of the anisotropy of H_{c2}. (b) Numerical fit to $H_{c2}(\theta)$ at 22 K and 32 K with the same parameters used to fit $H_{c2}(T)$. From the fit, the diffusivity values of D_1^{ab} =2.36 cm^2/s and D_2^{ab} =19.7 cm^2/s were obtained; the coupling parameters obtained from the fit are $L_{\sigma\sigma} \approx 0.810$, $L_{\pi\pi} \approx 0.285$, $L_{\sigma\pi} \approx 0.25$, and $L_{\pi\sigma} \approx 0.18$, respectively, close to the values obtained from ab-initio calculations (Ref. 34). The uncertainty of the fit parameters is no more than 5%, which is smaller than our experimental errors of 10%.

$a_0 = 2w/L_0$, $L_0 = \sqrt{(L_-^2 + 4L_{12}L_{21})}$, $L_\pm = L_{11} \pm L_{22}$, $w = L_{11}L_{22} - L_{12}L_{21}$, $t = T/T_c$, $\eta = D_2/D_1$, and $h = H_{c2}D_1/2\Phi_0 T$. Φ_0 is a single magnetic flux quantum, and D_1 and D_2 are the intraband diffusivities. The angular-dependent diffusivities $D_1(\theta)$ and $D_2(\theta)$ for both bands are calculated using the following equation:

$$D_m(\theta) = \sqrt{D_m^{(a)2}\cos^2\theta + D_m^{(a)}D_m^{(c)}\sin^2\theta}. \qquad (2)$$

From equations (1) and (2), we can obtain $H_{c2}(T,\theta)$.

The diffusivity D_1^c along the c axis is smaller than the in-plane diffusivity D_1^{ab} in MgB_2 due to the nearly 2D nature of the σ band. On the other hand, the values of D_2^c and D_2^{ab} do not differ substantially because of the isotropic 3D nature of the π band. The resulting relations among diffusivities are $D_1^c \ll D_1^{ab}$ and $D_2^c \approx D_2^{ab}$, which leads to the anomalous behavior of the anisotropy of $H_{c2}(T)$. The in-plane diffusivity ratio D_1^{ab}/D_2^{ab} is an important parameter in the equation (1).

We performed a numerical fit to three sets of transport data such as $H_{c2}(T)$ at θ =0°, $H_{c2}(\theta)$ at $T = 22$ K, and $T = 32$ K using the equations (1) and (2), shown in Fig. 3. The relation between the best fit intraband diffusivities in the σ and π bands is $D_2^a = 8.5 \times D_1^a$. This large $\eta = 8.5$ is consistent with the absence of a sharp upward curvature in $H_{c2}^{\parallel c}(T)$ at low T (see Fig. 1 in Ref. [2]), frequently observed in C-doped MgB_2 with extremely high H_{c2}. The inset of Fig. 3(a) shows the anisotropy $\gamma_{H_{c2}}(T)$ as a function of T. Again, this behavior is qualitatively consistent with that expected for $\eta \gg 1$, see Fig. 3(c) in Ref. [2]. The superconducting critical field, $H_{c2}^{\parallel c}(0)$, for field applied parallel to the c axis, obtained from the fit, equals 10 T. This indicates the presence of strong multiple intraband scattering channels. The value of in-plane intraband diffusivity ratio $\eta = 8.5$ provides information about the type of the intraband scatterers. The larger value of η, (smaller value of D_1^a) indicates the weakening of the 2D σ band by certain types of impurities, such as C and N. These impurities affect the 2D landscape by

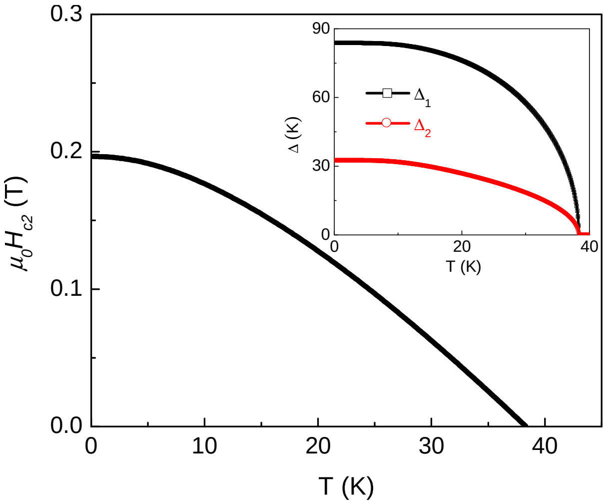

FIG. 4: (Color online) The calculated thermodynamic critical field H_c from the gap equations for two-band superconductors. The inset shows the calculated gap values from the two band model.

replacing p_{xy} orbitals of boron, and making the system more isotropic. The large value of D_2^a compared to D_1^a is also in good agreement with results from the α model,[10] and is the result of a large contribution of the π band to the total density of states.

C. λ and H_c from the two-band model

We calculated λ using the parameters obtained from the $H_{c2}(T,\theta)$ fit and the band calculations. The London equation for a two-gap superconductor is given by $\nabla \times (\lambda_L^2 \nabla \times \mathbf{H}) + \mathbf{H} = 0$, where the London penetration depth is $\lambda_L^{-2}(T) = \pi e^2 \mu_0 (N_1 D_1^{ab} \Delta_1 \tanh \frac{\Delta_1}{2T} + N_2 D_2^{ab} \Delta_2 \tanh \frac{\Delta_2}{2T})$: Indices of 1 and 2 represent the σ band and the π band, respectively. N_1 and N_2 are the electron densities of states. Δ_1 and Δ_2 are the gap magnitudes. D_1^{ab} and D_2^{ab} are the intraband diffusivities.[2] Using D_1^{ab} =2.36 cm^2/s, D_2^{ab} = 19.7 cm^2/s, obtained from the fit of $H_{c2}(T,\theta)$, $\Delta_1(0) = 84$ K, $\Delta_2(0) = 33$ K, obtained from the gap Eqs. (3), $N_1 = 0.3$ states/a^{3}eV, and $N_2 = 0.41$ states/a^{3}eV with a unit cell volume of a^3= 87.2 Å^{3}[14] (obtained from the band calculations),[34] we obtain $\lambda_L(0) \approx$170 nm, consistent with the measured value of $\lambda_{ab}(0)$ =200±30 nm. The calculated $\lambda_L(T)$ is shown as the blue curve in Fig. 2(b), consistent with the MFM experiment. This indicates that the two independent measurements of $\lambda(T)$ (MFM) and $H_{c2}(T)$ (transport) in MgB_2 are complementary for investigating superconducting properties.

The thermodynamic critical field (H_c) in MgB_2 is important for technological applications.[12] We evaluate H_c using the band coupling parameters, obtained from $H_{c2}(T,\theta)$, and the electron density of states obtained from the band calculations.

The gap equations for two-band superconductors[35] are

$$\hat{g} \begin{pmatrix} \Delta_1 \\ \Delta_2 \end{pmatrix} - \begin{pmatrix} N_1(0)\Delta_1 Y(\Delta_1) \\ N_2(0)\Delta_2 Y(\Delta_2) \end{pmatrix} = 0, \qquad (3)$$

with $Y(\Delta_j) = \int_0^{\omega_c} d\xi \frac{1}{\sqrt{(\xi^2+|\Delta_j|^2)}} \tanh\left[\frac{\sqrt{\xi^2+|\Delta_j|^2}}{2k_B T}\right]$, where $\hat{g}$ is the superconducting coupling matrix with $g_{11} = N_1 L_{22}/w, g_{12} = g_{21} = N_1 L_{12}/w = N_2 L_{21}/w$, and $g_{22} = N_2 L_{11}/w$. ω_c is some unknown cutoff frequency obtained from Eqs. (3) using the T_c obtained from the transport data. Using the parameters obtained from the fit of $H_{c2}(T,\theta)$, we have the superconducting coupling matrix, $\hat{g} = \begin{pmatrix} 0.46 & -0.40 \\ -0.40 & 1.78 \end{pmatrix} / (a^3 \mathrm{eV})$. The free energy is calculated[35] as $\mathcal{F} = \sum_{\mathrm{ij}} (\Delta_i g_{\mathrm{ij}} \Delta_j^*) - \frac{4}{\beta} \sum_i N_i \int_0^{\omega_c} d\xi \ln\left(\frac{\cosh\left(\frac{1}{2}\beta\sqrt{|\Delta_i|^2+\xi^2}\right)}{\cosh\left(\frac{1}{2}\beta\xi\right)}\right)$. Then H_c is given by $H_c^2/8\pi = -\mathcal{F}$. We calculate $\Delta_1(T)$ and $\Delta_2(T)$ as shown in Fig. 4 (inset). The calculated gap values at zero temperature are $\Delta_1(0) = 84$ K and $\Delta_1(0) = 33$ K, which are slightly larger than reported values.[10] The thermodynamic critical field at zero temperature, calculated from the two-band model, is approximately 2000 Oe. This value is smaller than those previously obtained in polycrystalline MgB_2 by specific heat measurements[36] and the values reported in clean single crystals.[37,38]

As discussed earlier, the superconducting properties in multiband superconductors are affected by the interactions among the bands.[37] We obtain $\xi_{ab}(0) = 5.7$ nm using $H_{c2}(0) = \Phi_0/2\pi\xi^2(0)$ and our experimental value $H_{c2}^{\parallel c}(0) = 10$ T. We can then use the Ginzburg-Landau theory to estimate the thermodynamic critical field in the film, $H_c = \Phi_0/2\sqrt{2}\pi\lambda(0)\xi(0) = 2100 \pm 300$ Oe. This value is close to the calculated value of $H_c = 2000$ Oe from the two band model. This suggests that the strong intraband scattering in the 3D π band makes the system more isotropic, and thus the system shows single band characteristics.

IV. CONCLUSION

In conclusion, we have measured $\lambda_{ab}(T)$ and $H_{c2}(T,\theta)$ in a MgB_2 film. Our analysis of $H_{c2}(T,\theta)$ shows that the large value of the in-plane intra-band diffusivity in the 3D π band is due to the presence of non-magnetic impurities such as C and N, indicating the system is more isotropic, which is partly responsible for a large λ. We calculated λ and H_c employing the gap equations for the two-band superconductors using the parameters obtained from $H_{c2}(T,\theta)$ and derived from band calculations. The calculated $\lambda_L(0) \approx 170$ nm is close to the measured $\lambda(0) = 200 \pm 30$ nm in MgB_2 film, indicating that two independent measurements, such as MFM and transport, are complementary, and provides a venue for thoroughly investigating superconducting properties.

The determination of $H_c(T)$ in clean MgB_2 and in multiband superconductors in general is a fascinating problem with both fundamental and technological relevance.

We acknowledge valuable discussions and communication of data with A. Gurevich. This work was supported by the US Department of Energy, Basic Energy Sciences, Division of Materials Sciences and Engineering, at Los Alamos. Work at Brookhaven was supported by the US Department of Energy under Contract No. DE-AC02-98CH10886. N.H. is member of CONICET (Argentina).

---

* Corresponding author: jeehoon@lanl.gov

[1] J. Nagamatsu, N. Nakagawa, T. Maranaka, Y. Zenitani, and J. Akimitsu, Nature **410**, 63 (2001).
[2] A. Gurevich, Phys. Rev. B. **67**, 184515 (2003).
[3] V. G. Kogan, C. Martin, and R. Prozorov, Phys. Rev. B. **80**, 014507 (2009).
[4] U. Welp, A. Rydh a, G. Karapetrov, W. K. Kwok, G. W. Crabtree, C. Marcenat, L. M. Paulius, L. Lyard, T. Klein, J. Marcus, S. Blanchard, P. Samuely, P. Szabo, A.G.M. Jansen, K.H.P. Kim, C. U. Jung, H.-S. Lee, B. Kang, and S.-I. Lee. Physica C **385**, 154 (2003).
[5] P. Samuely, P. Szabo, J. Kacmarcik, T. Klein, and A. G. M. Jansen, Physica C **385**, 244 (2003).
[6] B. J. Senkowicz, J. E. Giencke, S. Patnaik, C. B. Eom, E. E. Hellstrom, and D. C. Larbalestier, Appl. Phys. Lett. **86**, 202502 (2005).
[7] A. Matsumoto, H. Kumakura, H. Kitaguchi, B. J. Senkowicz, M. C. Jewell, E. E. Hellstrom, Y. Zhu, P. M. Voyles, and D. C.Larbalestier, Appl. Phys. Lett. **89**, 132508 (2006). A. Serquis, G. Serrano, M. S. Moreno, L. Civale, B. Maiorov, F. Balakirev, and M. Jaime, Supercond Sci. Technol. **20**, L12 (2007).
[8] V. Braccini *et al.*, Phys. Rev. B. **71**, 012504 (2005).
[9] V. G. Kogan, Phys. Rev. B. **66**, 020509(R) (2002).
[10] J. D. Fletcher, A. Carrington, O. J. Taylor, S. M. Kazakov, and J. Karpinski, Phys. Rev. Lett. **95**, 097005 (2005).
[11] M. Tinkham, *Introduction to Superconductivity* (McGraw Inc., NY, 1975).
[12] E. W. Collings, M. D. Sumption, and T. Tajima, Supercond. Sci. Technol. **17**, S595 (2004).
[13] A. Gurevich, Appl. Phys. Lett. **88**, 012511 (2006).
[14] X. X. Xi, Rep. Prog. Phys. **71**, 116501 (2008).
[15] A. A. Golubov, A. Brinkman, O. V. Dolgov, J. Kortus, and O. Jepsen, Phys. Rev. B **66**, 054524 (2002), and references therein.
[16] T. Dahm and D. J. Scalapino, Appl. Phys. Lett. **85**, 4436 (2004).
[17] X. K. Chen, M. J. Konstantinović, J. C. Irwin, D. D. Lawrie, and J. P. Franck, Phys. Rev. Lett. **87**, 157002 (2001).
[18] K. H. Lee, K. H. Kang, B. J. Mean, M. H. Lee, and B. K. Cho, J. Magnet. Magnet. Mater. **272**, 165 (2004).
[19] F. Simon *et al.*, Phys. Rev. Lett. **87**, 047002 (2001).
[20] D. K. Finnemore, J. E. Ostenson, S. L. Bud′ko, G. Lapertot, and P. C. Canfield, Phys. Rev. Lett. **86**, 2420 (2001).
[21] B. H. Moeckly and W. S. Ruby, Supercond. Sci. Technol. **19**, L21 (2006).
[22] Lin Gu, Brian H. Moeckly, and David J. Smith, Journal of Crystal Growth **280**, 602 (2005).
[23] E. Nazaretski, K. S. Graham, J. D. Thompson, J. A. Wright, D. V. Pelekhov, P. C. Hammel, and R. Movshovich, Rev. Sci. Instrum. **80**, 083074 (2009).
[24] A SSS-QMFMR cantilever, Nanosensors, Inc.
[25] J. Kim *et al.* (unpublished).
[26] J. Kim, F. Ronning, N. Haberkorn, L. Civale, E. Nazaretski, N. Ni, R. J. Cava, J. D. Thompson, and R. Movshovich, Phys. Rev. B **85**, 180504(R) (2012).
[27] J. H. Xu, J. H. Miller, and C. S. Ting, Phys. Rev. B **51**, 424 (1995).
[28] Q. Lu, K. Mochizuki, J. T. Markert, and A. de Lozanne, Physica C **371**, 146 (2002).
[29] O. M. Auslaender, L. Luan, E. W. J. Straver, J. E. Hoffman, N. C. Koshnick, E. Zeldov, D. A. Bonn, R. Liang, W. N. Hardy, and K. A. Moler, Nature Phys., **5** 35 (2009).
[30] E. W. J. Straver, J. E. Hoffman, O. M. Auslaender, D. Rugar, and Kathryn A. Moler, Appl. Phys. Lett. **93**, 172514 (2008).
[31] T. Shapoval, H. Stopfel, S. Haindl, J. Engelmann, D. S. Inosov, B. Holzapfel, V. Neu, and L. Schultz, Phys. Rev. B **83**, 214517 (2011).
[32] L. Luan, O. M. Auslaender, T. M. Lippman, C. W. Hicks, B. Kalisky, J. H. Chu, J. G. Analytis, I. R. Fisher, J. R. Kirtley, and K. A. Moler, Phys. Rev. B **81**, 100501(R) (2010).
[33] G. K. Perkins, J. Moore, Y. Bugoslavsky, L. F. Cohen, J. Jun, S. M. Kazakov, J. Karpinski, and A. D. Caplin, Supercond. Sci. Technol. **15**, 1156 (2002).
[34] A. A. Golubov, J. Kortus, O. V. Dolgov, O. Jepsen, Y. Kong, O. K. Andersen, B. J. Gibson, K. Ahn, and R. K. Kremer, J. Phys.: Condens. Matter **14**, 1353 (2002).
[35] S.-Z. Lin and X. Hu, Phys. Rev. Lett. **108**, 177005 (2012).
[36] Y. X. Wang, T. Plackowski, and A. Junod, Physica C **355**, 179 (2001).
[37] F. Bouquet, R. A. Fisher, N. E. Phillips, D. G. Hinks, and J. D. Jorgensen, Phys. Rev. Lett. **87**, 047001 (2001).
[38] M. Zehetmayer, M. Eisterer, J. Jun, S. M. Kazakov, J. Karpinski, A. Wisniewski, and H. W. Weber, Phys. Rev B **66**, 052505 (2002).